Indian Journal of Engineering & Materials Sciences
Vol. 30, October 2023, pp. 676-680
DOI: 10.56042/ijems.v30i5.6852

Investigation of α-Fe_2O_3 and Cr doped α-Fe_2O_3 Based Nano-Film as Resistive Switching Material for ReRAM Device Application

Neeraj Dhariwal, Preety Yadav, Manju Kumari, Vinod Kumar*, & O P Thakur

Material Analysis and Research Laboratory, Department of Physics, Netaji Subhas University of Technology, New Delhi 110 078, India

Received: 9 August 2023; Accepted: 26 September 2023

Ferric oxide (α-Fe_2O_3) based nanoparticles show a vast number of applications along with resistive switching. In the recent study, we synthesized α-Fe_2O_3 nanoparticles and Cr^{3+} doped α-Fe_2O_3 to see the variation in the resistive switching property with chromium doping. XRD and FESEM characterizations have been carried out to confirm the structural and morphological properties of both α-Fe_2O_3 and $CrFeO_3$ nanoparticles. Optical study has been done by using UV-visible spectroscopy and a decrease in band gap was observed with the chromium doping. I-V characteristics have been studied at room temperature for the synthesized material. The resistive switching effect for synthesized material is confirmed by applying negative and positive bias voltage for which current shows different values. $CrFeO_3$ shows a larger loop of hysteresis as compared to α-Fe_2O_3 confirming a better material for ReRAM application.

Keywords: Nano-film, Nanoparticle, Resistive switching, Spectroscopy

1 Introduction

The constant demand for higher performance and lower power consumption in electronic devices has led to the development of new materials and technologies. Resistive random access memory (ReRAM) is a promising technology that has attracted significant attention due to its potential for high-density storage, low power consumption, and fast access time[1, 2]. One of the critical components of ReRAM devices is the resistive switching material, which allows for reversible switching between high and low resistance states. Various materials such as metal oxides, nano-composites and perovskites have been tried[3-5] to improve storage. Iron oxide is a non-toxic, water soluble and eco-friendly material. It's amazing optical, dielectric and memory storage properties make it a very useful material[6-8].

In this context, α-Fe_2O_3 based nano-films have emerged as a promising candidate for resistive switching material due to their unique properties such as high surface area, tuna ble conductivity, and easy synthesis. In this investigation, the α-Fe_2O_3 and Cr-doped α-Fe_2O_3 based nano-film have been explored as a resistive switching material for ReRAM device application, with a focus on optimizing its performance for practical applications. The results of this study have the potential to advance the development of ReRAM devices and contribute to the field of advanced electronic materials.

2 Materials and Methods

2.1 Synthesis

In this present work, α-Fe_2O_3 and Cr doped α-Fe_2O_3 have been synthesized using hydrothermal route without using any precipitating agent as shown in Fig. 1. $Fe(NO_3)_3.9H_2O$ and $Cr(NO_3)_3.6H_2O$ were mixed individually into de-ionised water in a stoichiometric ratio for a duration of 30 minutes at room temperature (30 °C). Afterwards, both the solutions were mixed together for 1 hour with gentle

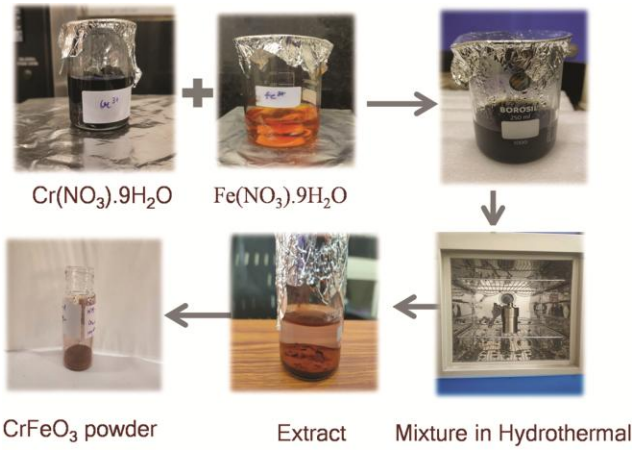

Fig. 1 — Synthesis of Cr-doped α-Fe_2O_3 using hydrothermal.

*Corresponding author (E-mail: vinod@nsut.ac.in)

heating at 60 °C and further transferred into an autoclave with an operating temperature of 150 °C for duration of 5 hours. After room temperature cooling of autoclave, the precipitates were extracted and washed using de-ionised water. The obtained precipitates were then dried at 100 °C for 2 hours in vacuum oven.

2.2 Characterization

To investigate the structural parameters, X-ray diffraction (XRD) was used with a scan range of 10-80 degrees and morphological analysis was obtained from the FESEM (Field Emission Scanning Electron Microscope) characterization. To know more about the successful doping of chromium into α-Fe_2O_3 along with the bond formation, FTIR (Fourier Transform Infrared Spectroscopy) analysis was employed. While for investigating the resistive switching behavior of the synthesized nanoparticles I-V characterization was used.

2.3 Fabrication

FTO coated glass substrate was taken for the deposition of developed nanomaterial. Firstly, the substrate was cleaned using acetone and then rinsed with de-ionised water. Then, the developed nanomaterial was deposited over it using blade coating technique and allowed to dry in vacuum oven at 80 °C for 2 hours. Finally, silver (Ag) epoxy was deposited over the fabricated iron oxide thin film as a top electrode and cured for 20 minutes at 100 °C.

3 Results and Discussion

3.1 Structural analysis and phase identification

Figure 2 shows the XRD pattern of synthesized α-Fe_2O_3 and Cr doped α-Fe_2O_3 with the phase determination. As, with the doping of chromium no extra peak was observed, but shift in peak towards higher degree of phase angle was seen. The diffraction angle in XRD is dependent of crystal lattice distance and its position[9]. Analyzing the data, Rhombohedral structure was obtained and crystallite size was calculated using the eq.(1).

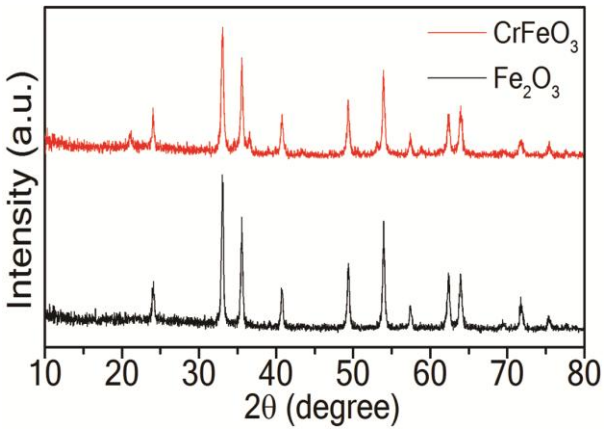

Fig. 2 — X-ray diffraction (XRD) pattern of α-Fe_2O_3 and Cr doped α-Fe_2O_3.

$$D = \frac{K\lambda}{\beta Cos\theta} \quad \ldots (1)$$

Where K is the sherrer's constant, wavelength of Cu-Kα radiation i.e. λ and θ_{104} is the Bragg's angle for plane 104.

Decrease in crystallite size was found with the doping of chromium, which is due to the introduction of lattice strain and lattice structure distortion, hindering the growth of larger crystallites. Also, the obtained results were used to calculate the porosity of the nanomaterials as shown in Table 1 using eq.(2)

$$P = 1 - \frac{p_{exp}}{p_{XRD}} \quad \ldots (2)$$

Where, p_{exp} is the true density and p_{XRD} is the X-ray density. The developed lattice strain in nanomaterial, which also affects the crystallite size, is calculated using W-H equation[10]

$$\beta cos\theta = \frac{K\lambda}{D} + 4\mathcal{E}sin\theta \quad \ldots (3)$$

Figure 3 shows the W-H plot of α-Fe_2O_3 and Cr doped α-Fe_2O_3. The slope of linear fit results in the value of developed strain.

3.2 Study of morphology

As most of the material property is dependent on its morphology. So, to know about the morphology of the developed nanomaterials FESEM characterization was employed. As shown in Fig. 4, we observed hike in the porosity of α-Fe_2O_3, which can be attributed to the fact that doping of chromium increases surface area and introduces the structural defects, which enhance the porosity of the material.

3.3 FTIR analysis

Figure 5 shows the FT-IR of both α-Fe_2O_3 and $CrFeO_3$ in the range of 400-4000 cm^{-1}. A broad peak observed between 3000-3657 cm^{-1} is for stretching vibration in O-H bond obtained from the intermolecular as well as intramolecular hydrogen

Table 1 — Various parameters obtained from XRD

Sample	Crystallite size (nm)	Strain (10^{-3})	Porosity
α-Fe_2O_3	25.83	3.4	0.22
$CrFeO_3$	20.44	3.8	0.39

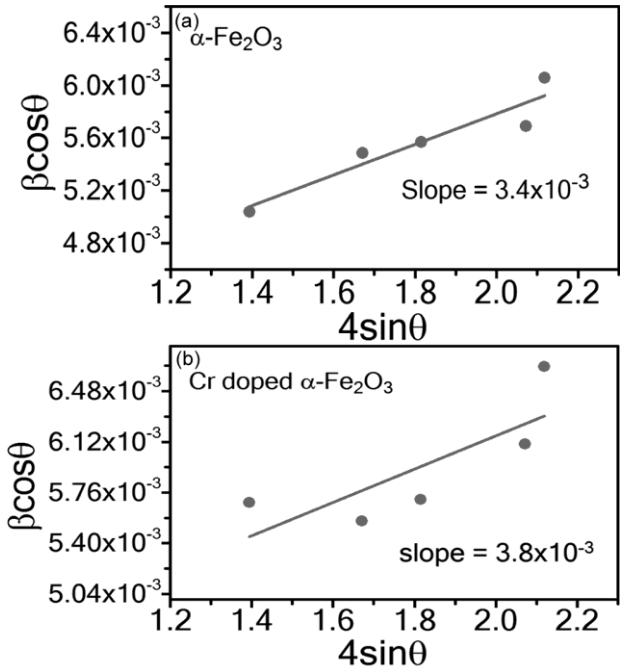

Fig. 3 — W-H plot with linear curve fitting.

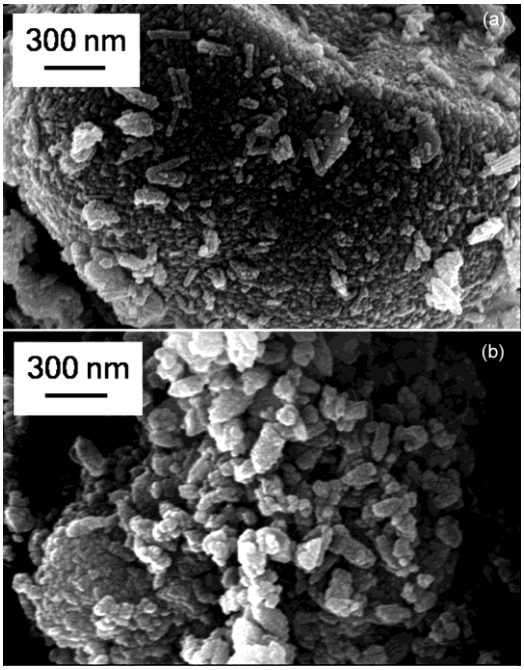

Fig. 4 — Field Emission Scanning Electron Microscope (FESEM) images of (a) α-Fe_2O_3, & (b) $CrFeO_3$.

bonding[11]. The presence of O-H group was also observed at approximately 1330 cm^{-1}. The observed peaks at ~423 cm^{-1} and ~520 cm^{-1} are linked with the vibration mode of Fe-O[12], while peaks at ~800 cm^{-1} and ~900 cm^{-1} are associated with the Cr=O stretching. And a peak of CO_2 was also revealed at

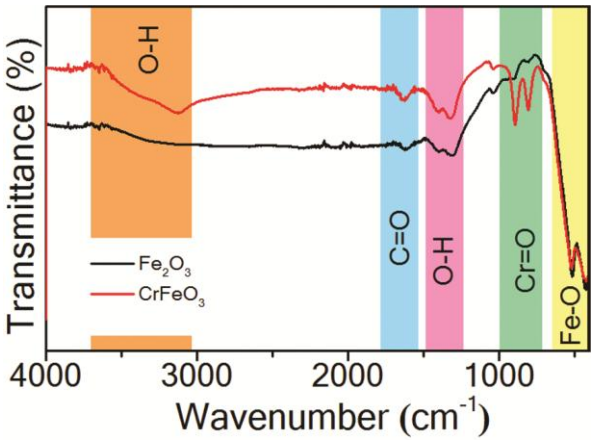

Fig. 5 — Fourier Transform Infrared Spectroscopy (FTIR) spectra of (a) α-Fe_2O_3, & (b) $CrFeO_3$.

1620 cm^{-1}. The results obtained from the FT-IR data also confirmed the successful doping of chromium in α-Fe_2O_3.

3.4 I-V characteristics

I-V characteristics of bipolar resistive switching device have been shown in Fig. 6. In case of α-Fe_2O_3, we observed a small change in $\frac{R_{off}}{R_{on}} = 4$ and memory loss was also seen. While, in case of Cr doped α-Fe_2O_3, when a voltage sweep (0-6 V) was applied, current from its initial state increased to I_C = 7.33 A at a set voltage of V_S = 5 V with $\frac{R_{off}}{R_{on}} = 80$. As a result of this, RS device switches from HRS to LRS. The state of LRS remained same upto 0V. When the sweep voltage reached to V_{RS} ~ 6V, change in device state to HRS was observed. This significant improvement in I-V characteristics with the Cr^{3+} ion doping can be attributed to the fact that, porosity caused by Cr^{3+} ion implantation creates the interconnected voids which contributes to the ion migration during RS process. Also, the improved surface area helps in dissolution of conductive filament, which is mainly responsible for the change in resistance in RS devices. The results obtained from I-V characteristics showed the bipolar bi-stable resistive switching behavior.

3.5 Mechanism

Mechanism of resistive memory function can be interpretated using ion migration as in Fig. 7[13]. Initially, top Ag coated top electrode is biased with positive voltage suppy, while FTO coated glass was given negative voltage with a voltage sweep of -6V to +6V. As the applied voltage increase, an increase in

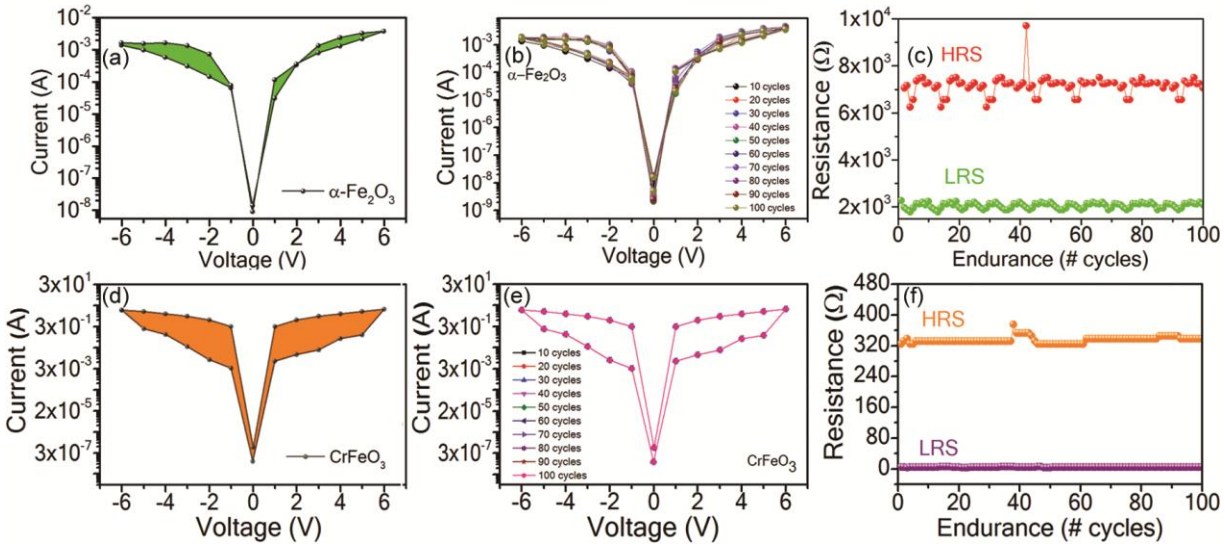

Fig. 6 — I-V characteristics of α-Fe_2O_3, Cr doped Fe_2O_3 and endurance test for 100 cycles to check device stability.

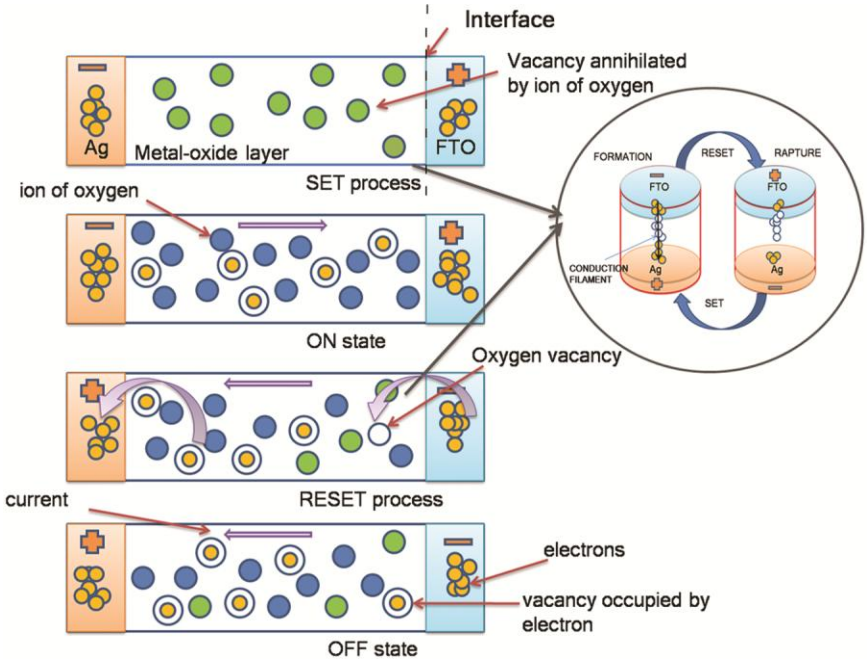

Fig. 7 — Schematic illustration of resistive switching mechanism.

Ag^+ ions was observed with the increase in force of repulsion between multiple Ag^+ ions. While, in iron oxide film, concentration of O_2^- also increases with applied voltage, resulting in upward movement of O_2^- ion, due to the generated vacancies of negative charge ion in α-Fe_2O_3 were used by Ag^+ ions as a trap charge and a consequence of that is the formation of filament within the top electrode and the bottom electrode. As a result of this, the HRS state of the memory device changes to LRS and goes into a SET process. So, as to achieve initial state, a reverse voltage sweep from -6V to +6V is applied to both top and bottom electrode. A reverse process of ion migration occurs and filaments starts to decrease and resistive memory device undergo HRS.

The charge trapping mechanism was taken into consideration to explain about the conduction mechanism of FTO/Fe_2O_3/Ag[14] as in Fig. 8.

In voltage range from -6V to +6V, HRS state of memory device continuous due to low amount of charge carriers. HRS is further classified into two categories namely (i) ohmic region (I α V), with a

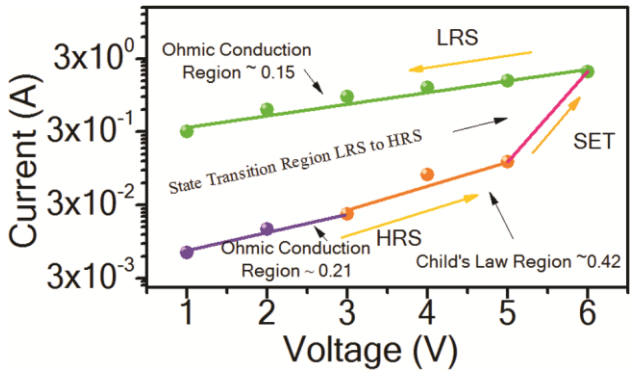

Fig. 8 — Mechanism of charge trapping.

slope fitting of ~ 0.15, and (ii) child's law region, slope of ~ 0.42. In child's region, we observe an increase in current with applied voltage. Also, a sudden increase in current and state changes from HRS to LRS have been observed at a threshold voltage of 5V, ($I \alpha V^n$) as shown in Fig. 8.

After that, when reverse voltage was applied from +6V to -6V, device follows the same pattern of ohmic conduction region and at -6V, developed filament vanishes and state changes from LRS to HRS due to low charge carriers in active layer. The stability of device is an important aspect. Room temperature stability of FTO/Fe_2O_3/Ag resistive switching devices were studied for continuously 100 cycles as depicted in Fig. 6 which also confirms the continuous stability in HRS and LRS by Cr doping in α-Fe_2O_3 with an increase in R_{off}/R_{on} ratio of ~ 80 as shown in Fig. 8.

4 Conclusion

In this study, α-Fe_2O_3 and Cr-doped α-Fe_2O_3 have been synthesized using hydrothermal method without any precipitating agent. Furthermore the material has been coated on FTO using blade coating method. The ratio of R_{off}/R_{on} significantly increased from 4 to 80 times with the doping of chromium ion. Also, Cr doped iron oxide based film shows fast resistive switching. The proposed resistive switching device shows long retention performance and stable endurance for 100 cycles, which shows its high reliability in various memory storage devices. The device proposed in this study opens the doors for various advanced application in memory storage.

Reference

1 Zhang Y, Poddar S, Huang H, Gu L, Zhang Q, Zhou Y, Yan S, Zhang S, Song Z, Huang B, Shen G, and Fan Z, *Sci Adv*, 7 (2021) 36.
2 Mikolajick S S M, *Nat Nanotechnol*, 30 (2019) 25.
3 Gao S, Yi X, Shang J, Liu G and Li R W, *Chem Soc Rev*, 48 (2019) 1531.
4 Fukuchi A T, Nakagawa R, Arita M and Takahashi Y, *ACS Appl Mater Interfaces*, 10 (2018) 5609.
5 Guan X, *Adv Funct Mater*, 28 (2018) 1.
6 Dadashi S, Poursalehi R, and Delavar H, *Procedia Materials Science*, 11 (2015) 722.
7 Kumar DS, Chandra Babu Naidu K, Rafi MM, Prem Nazeer K, Begam AA, Kumar GR**,** *Mater Sci Pol*, 36(1), 2018, 123.
8 Nguyen HH, Kieu H, Ta T, Park S, Phan TB, and Pham NK, *RSC Adv*, (2020) 12900.
9 T P S July, *IEEE Trans Plasma Sci*, 46 (2019) 4111.
10 Dhariwal N, Chahar M, Kumar V, and Thakur OP, *Sens Actuators B Chem*, 390 (2023) 1.
11 Yadav P, Dhariwal N, Kumari M, Kumar V, and Thakur OP, *Chemosphere* , 343 (2023) 140208.
12 Suresh R, Giribabu K, Manigandan R, Mangalaraja RV, Solorza JY, Stephen A, Narayanan V, *Solid State Sci*, 63 (2017) 39.
13 Hassan G, Bae J, Umair M, and Ali S, *Mater Sci Eng B Solid State Mater Adv Technol*, 246 (2019) 1.
14 Khan MU, Hassan G, and Bae J, *Appl Phys A*, 125 (2019) 1.